Supporting Information

Rybicka et al. 10.1073/pnas.0914867107

SI Materials and Methods

Mice and Cells. C57BL/6 mice were purchased from Charles River Laboratories. The congenic mouse strains B6.129S6-Cybb$^{-/-}$ (Cybb$^{-/-}$) and B6.129P2-Nos2$^{-/-}$ (iNOS$^{-/-}$) were purchased from Jackson Laboratories. All animal experiments were conducted according to protocols approved by the University of Calgary Animal Use and Care Committee. BMMØs were derived from bone marrow as previously described (1). For fluorometric phagosomal analysis, fully differentiated BMMØs were seeded in μ-clear 96-well plates (Greiner Bio-One) and allowed 24 h to establish a confluent monolayer. Where indicated, bone marrow-derived murine macrophages (BMMØs) were preactivated with 100 U/mL of recombinant IFNγ (Peprotech) for 18 h. Treatment of BMMØs with diphenyleneiodonium (DPI; 0.5 μM) (EMD Chemicals), 3,3′,4′-trihydroxyflavone (THF; 10 μM) (Indofine Chemical), quercetin (25 μM) (EMD Chemicals), or dimethyl sulfoxide (DMSO) occurred over 1 h preceding phagocytosis of experimental particles unless otherwise stated.

Live-Cell Fluorometric Phagosomal Analysis. Fluorescently labeled, IgG-coupled 3-μm silica particles were prepared as previously detailed (2–4) and used for phagosomal lumenal characterization in live BMMØs (1, 3, 4). Measurements were performed in microplate format using a FLUOstar Optima fluorescent plate reader (BMG Labtech) at 37 °C, at an MOI of 1–2 particles/BMMØ, in an assay buffer consisting of phosphate-buffered saline supplemented with 1 mM $CaCl_2$, 2.7 mM KCl, 0.5 mM $MgCl_2$, 5 mM dextrose, and 0.25% gelatin. Phagosomal pH was calculated by recording the ratio of the fluorescent emission of carboxyfluorescein succinimidyl ester excited at 450 nm and 490 nm followed by polynomial regression to a standard curve generated using experimental particles in buffers of known pH (4). Phagosome-lysosome communication was evaluated by measuring the fluorescence resonance energy transfer (FRET) efficiency between a particle-restricted donor fluor (Alexa Fluor 488 succinimidyl ester; Molecular Probes) and a fluid-phase acceptor fluor (Alexa Fluor 594 hydrazide; Molecular Probes) that had been previously pulsed and chased into lysosomes over a period of 18 h (5, 6). The oxidative burst was evaluated by measuring the fluorescence following oxidation of H2HFF-OxyBURST substrate (Molecular Probes) relative to the calibration fluor Alexa Fluor 594 succinimidyl ester (2). The hydrolytic activities of phagosomal β-galactosidase, total proteases, cathepsin B/L, and cathepsin D/E were measured by recording the rate of substrate-liberated fluorescence relative to a calibration fluor, using 5-dodecanoylaminofluorescein di-β-D-galactopyranoside (Molecular Probes), DQ green Bodipy BSA (Molecular Probes), (biotin-LC-Phe-Arg)$_2$-rhodamine 110 (kindly donated by David Russell, Cornell University, Ithaca, NY), and Mca-GKPILFFRLK (Dnp)-r-NH$_2$ (Anaspec), respectively (3, 4). Relative fluorescent units (RFU) defined by the equation $RFU = SF_{RT}/CF_{RT}$ (where SF_{RT} = substrate fluorescence in real time and CF_{RT} = calibration fluorescence in real time) were plotted against time. For comparison of hydrolytic capacities across experiments, the gradients (as described by the equation $y = mx + c$, where y = RFU, m = gradient, and x = time) of the linear portion of the relative substrate fluorescence plotted against time were calculated relative to an appropriate internal control unless otherwise indicated. Experimental groups were compared by one-way analysis of variance (ANOVA) with Bonferroni's multiple comparison post-hoc test using GraphPad Prism software.

Measurement of Phagosomal Disulfide Reduction. The rates of phagosomal reduction of cystine (dimeric, oxidized form of two cysteine residues) were recorded by using a modified form of the self-quenched cystine-based fluorogenic substrate Bodipy FL L-cystine (Molecular Probes). This compound was modified through the available carboxylic acids in order for it to be covalently coupled to experimental particles. In brief, 0.5 mg of Bodipy FL L-cystine was reacted with 0.8 mg 1-ethyl-3-[3-dimethylaminopropyl]carbodiimide hydrochloride and 2.2 mg *N*-hydroxysulfosuccinimide in a buffer containing 100 mM 2 (*N*-morpholino)ethanesulfonic acid and 500 mM NaCl (pH 6) for 15 min (7, 8). The amine-reactive Bodipy FL L-cystine-(NHS ester)$_2$ product was separated by chromatography using carboxymethyl-cellulose and directly coupled to BSA and IgG bound to 3-μm silica beads in 0.1 M borate buffer (pH 8.0). The unreacted NHS ester groups on the corresponding cysteines were quenched with glycine (100 mM) (for a chemical structure, see Fig. S7). The particles were further derivatized with Alexa Fluor 594 succinimidyl ester to act as a calibration fluor. Following phagocytosis of the particles, reduction of the mixed disulfide of the bound substrate (resulting in the dequenching of the Bodipy FL fluorescence) was detected as an increase in fluorescent emission at 520 nm during excitation at 490 nm. Values were expressed relative to calibration fluorescence and plotted against time. For comparison of reductive capacities across experiments, the gradients of the linear portion of the resulting plots were calculated relative to those of untreated wild-type (WT) cells.

Phagosome Isolation and in Vitro Determination of Cathepsin Activities. Phagosomal isolation for detection of specific cathepsins by Western blotting was achieved through magnetic-assisted isolation of phagosomes containing IgG-coupled Dynabeads (Invitrogen) as previously described (9). For in vitro measurement of cathepsin activities, phagosomal isolation was performed using IgG-opsonized silica beads to avoid any potential Fenton chemistries created by iron-containing beads. In brief, 30 min after phagocytosis, BMMØs were scraped and plasma membrane was selectively lysed by nitrogen decompression (Parr Instruments) in homogenization buffer (250 mM sucrose, 0.5 mM EGTA, 0.5 mM EDTA, 20 mM sodium acetate, 0.05% gelatin) at pH 5.5. Phagosomes were enriched by centrifugation at 500 × *g* through a series of Ficoll gradients in low-pH buffers, enumerated, and standardized across samples. Half of each sample was incubated for 10 min on ice with 1 μM dihydrolipoic acid (DHLA) and 30 mM reduced glutathione (GSH). Fluorometric determination of cathepsins B, S, and D/E activities was achieved by incubation of 10^5–10^6 phagosomes in 0.1 M potassium acetate (pH 5.5) with 0.5% Nonidet P-40 containing 50 μM fluorogenic substrates Z-RR-MNA (Sigma), Ac-KQKLR-AMC (Anaspec), or Mca-GKPILFFRLK(Dnp)-r-NH$_2$ (Anaspec), respectively, using a FLUOstar Optima plate reader (BMG Labtech) at 37 °C. Gradients of the initial rate of reaction were determined by curve-fitting applications in Excel and expressed relative to phagosomes from untreated Cybb$^{-/-}$ BMMØs. Western blot determination of the proportion of active cathepsin B within the isolated phagosomes was achieved by incubation of the phagosomes with 10 μM irreversible cathepsin B inhibitor biotin-Phe-Ala-FMK (SM Biochemicals) for 15 min at pH 5.5, 37 °C, with agitation. The proportion of biotinylated (active) cathepsin B before and after reduction with DHLA and GSH was determined by Western blot.

1. Yates RM, Hermetter A, Russell DG (2005) The kinetics of phagosome maturation as a function of phagosome/lysosome fusion and acquisition of hydrolytic activity. *Traffic* 6:413–420.
2. VanderVen BC, Yates RM, Russell DG (2009) Intraphagosomal measurement of the magnitude and duration of the oxidative burst. *Traffic* 10:372–378.
3. Yates RM, Hermetter A, Russell DG (2009) Recording phagosome maturation through the real-time, spectrofluorometric measurement of hydrolytic activities. *Methods Mol Biol* 531:157–171.
4. Yates RM, Russell DG (2008) Real-time spectrofluorometric assays for the lumenal environment of the maturing phagosome. *Methods Mol Biol* 445:311–325.
5. Yates RM, Russell DG (2005) Phagosome maturation proceeds independently of stimulation of Toll-like receptors 2 and 4. *Immunity* 23:409–417.
6. Yates RM, Hermetter A, Taylor GA, Russell DG (2007) Macrophage activation downregulates the degradative capacity of the phagosome. *Traffic* 8:241–250.
7. Anjaneyulu PS, Staros JV (1987) Reactions of *N*-hydroxysulfosuccinimide active esters. *Int J Pept Protein Res* 30:117–124.
8. Carraway KL, Triplett RB (1970) Reaction of carbodiimides with protein sulfhydryl groups. *Biochim Biophys Acta* 200:564–566.
9. Ullrich HJ, Beatty WL, Russell DG (1999) Direct delivery of procathepsin D to phagosomes: Implications for phagosome biogenesis and parasitism by Mycobacterium. *Eur J Cell Biol* 78:739–748.

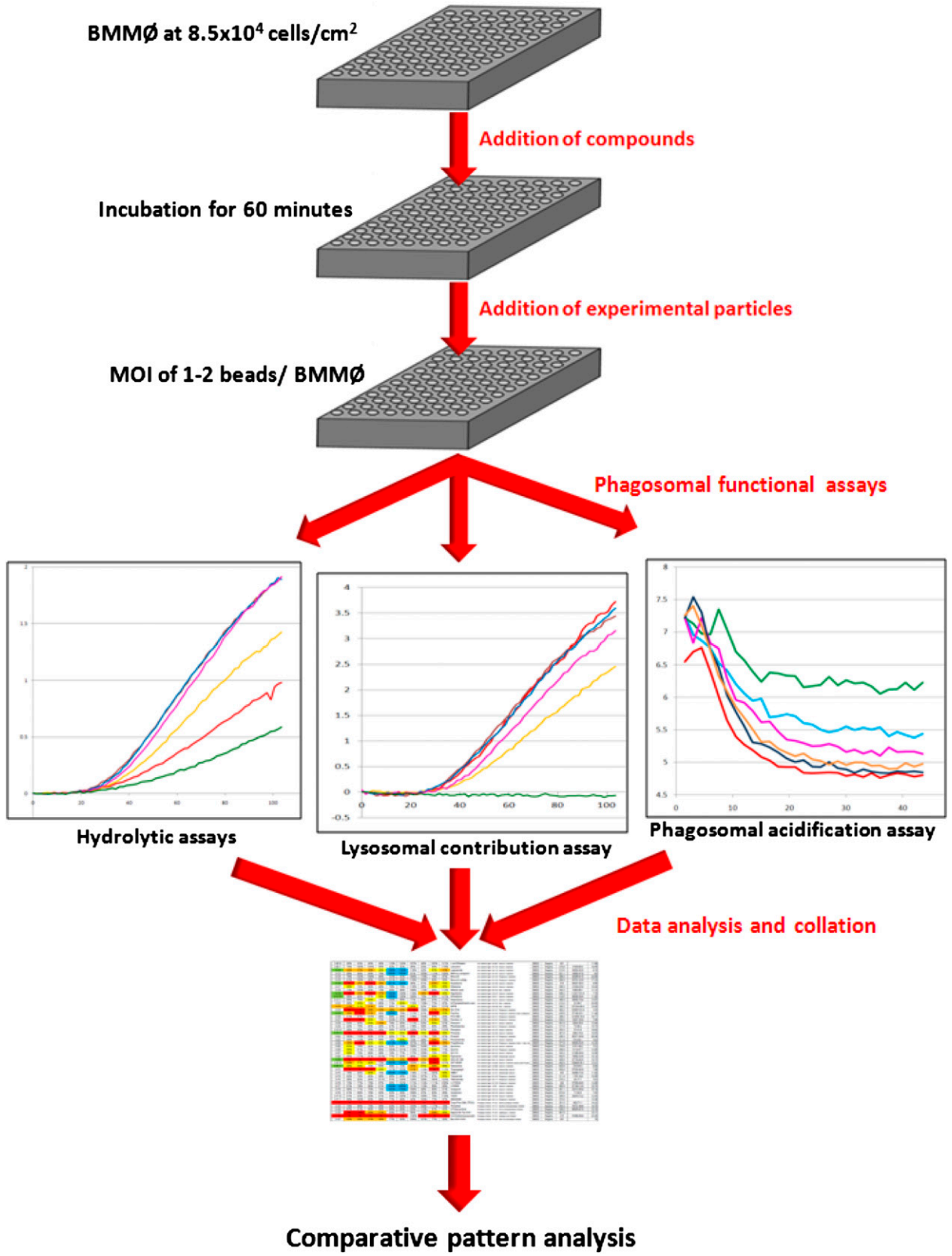

Fig. S1. A cell-based screening approach for exploration of the interconnectivity between phagosomal functional parameters. Modestly sized chemical libraries have limited application in large-scale discovery programs that use a single screening parameter, but can be used to great effect in combination with a bank of multiplexed assays and comparative analysis. This figure outlines an approach to explore the functional interconnectivity of the phagosomal physiology using bioactive chemical-based libraries and comparative analysis of functional parameters of the phagosome. It exploits a bank of live-cell fluorometric assays that report on maintenance or perturbation of phagosomal functions in the presence of a bioactive compound. In brief, confluent monolayers of BMMØs in multiwell plates are incubated with compounds for 1 h. Functionalized experimental particles are added and phagosomal parameters

Legend continued on following page

are recorded in real time using a fluorescence plate reader following their phagocytosis. Each phagosomal parameter is measured in duplicate or triplicate and analyzed with respect to DMSO-treated controls. Compounds that effect a change greater than two standard deviations from DMSO-treated controls for each parameter are flagged, and treated BMMØs are inspected for morphology, viability, and phagocytic index. Data from all assays are compiled according to compound. Pattern analysis to identify functional interconnectivity between phagosomal functions is performed by automated or manual means.

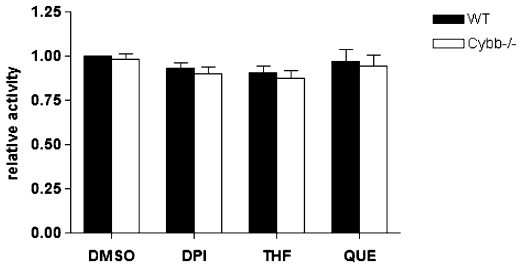

Fig. S2. Total proteolytic capacity of whole-cell lysates is equivalent between WT and Cybb$^{-/-}$ BMMØs. WT and Cybb$^{-/-}$ BMMØs with or without pretreatment with 0.5 μM diphenyleneiodonium (DPI), 10 μM trihydroxyflavone (THF), 25 μM quercetin (QUE), or DMSO alone for 1 h were lysed in lysis buffer (pH 5.5) containing 0.1% Triton X-100. Relative total proteolytic activities of the whole-cell lysates were determined by the rate of increase in fluorescence from soluble DQ-albumin at 37 °C, pH 5.5 and expressed relative to the corresponding WT-DMSO samples. Graph represents data from four independent experiments. Error bars denote standard error of the mean (SEM). No statistical significance between samples was found by ANOVA.

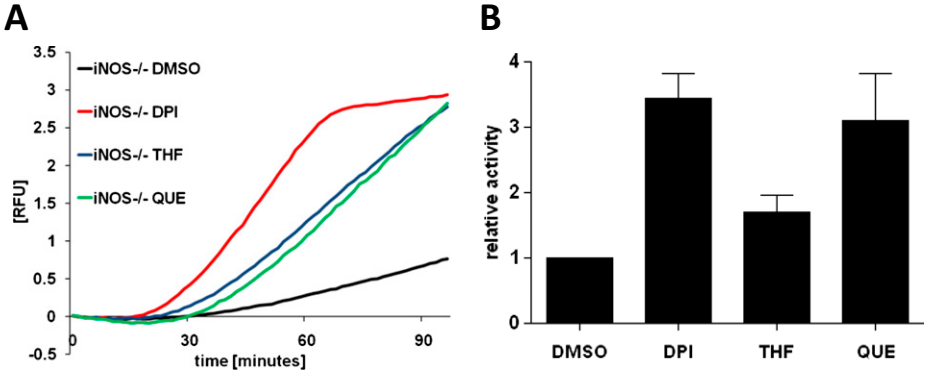

Fig. S3. NOX2-mediated inhibition of phagosomal proteolysis is independent of inducible nitric oxide synthase (iNOS). Phagosomal bulk proteolysis was assessed by measurement of fluorescence liberated through hydrolysis of particle-associated DQ-albumin relative to calibration fluorescence in IFNγ-activated iNOS$^{-/-}$ BMMØs. (*A*) Real-time representative traces. RFU = SF_{RT}/CF_{RT} (where RFU = relative fluorescent units, SF_{RT} = substrate fluorescence in real time, and CF_{RT} = calibration fluorescence in real time). (*B*) Relative rates/activities were determined through calculation of the gradient of the linear portion of the real-time trace (as described by $y = mx + c$, where y = relative fluorescence, m = gradient, and x = time) relative to DMSO-treated samples. Graph represents averaged data from two independent experiments. Error bars denote SEM.

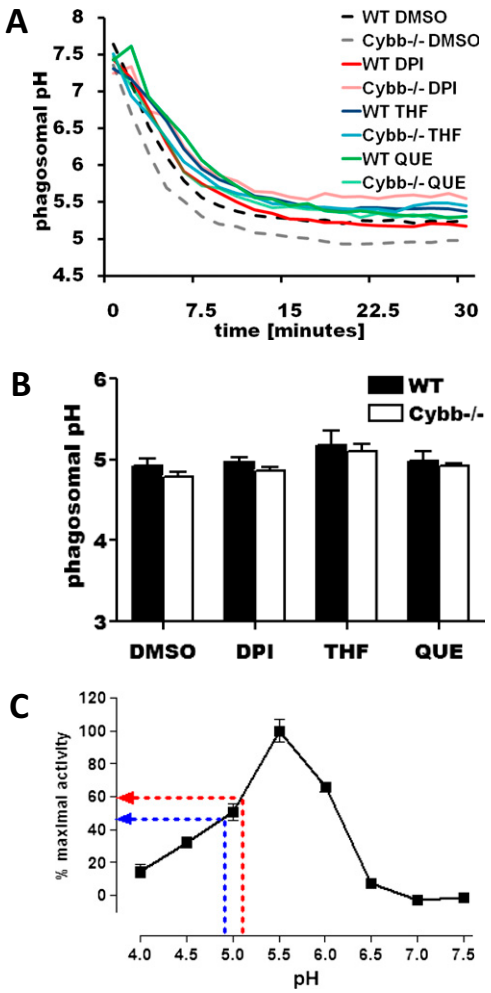

Fig. S4. An alkalinization of 0.13–0.18 pH units would theoretically increase, not decrease, the proteolytic efficiency of the phagosome. (*A* and *B*) Phagosomal pH following phagocytosis was calculated using excitation ratio fluorometry of the pH-sensitive carboxyfluorescein on IgG-coupled beads followed by regression to a standard curve. (*A*) Representative acidification profiles in IFNγ-activated BMMØs. (*B*) Final lumenal pH at 30 min postinternalization in IFNγ-activated BMMØs from four independent experiments. Error bars represent SEM. (*C*) To determine whether the difference of pH between WT and Cybb$^{-/-}$ phagosomes could account for the inhibition of phagosomal proteolysis, we regressed the pH values of phagosomes at 30 min from resting BMMØs against a proteolytic activity versus pH curve. This curve was generated by measuring proteolytic efficiency of magnetically isolated lysosomal extract of BMMØs using the fluorogenic substrate DQ-albumin in buffers of known pH. Theoretical change in proteolytic efficiency of lysosomal hydrolases corresponding to a phagosomal pH of resting WT (5.02) and Cybb$^{-/-}$ (4.85) BMMØs is represented by red and blue arrows, respectively.

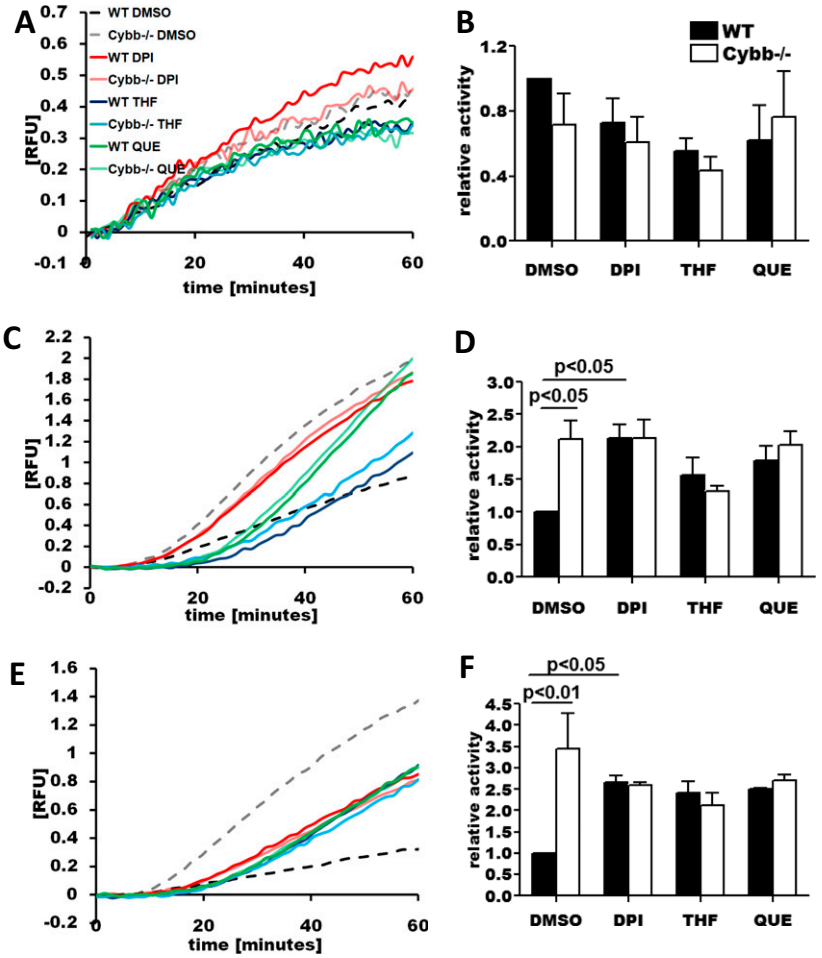

Fig. S5. NOX2 activity negatively regulates cysteine but not aspartic cathepsin activity in the phagosome. Complete real-time representative traces are from Fig. 3. Relative activities of phagosomal proteases were evaluated using cathepsin D/E- and B/L-specific fluorogenic peptides bound to IgG-coupled experimental particles in WT and Cybb$^{-/-}$ BMMØs in the presence or absence of DPI, QUE, or THF. (*A* and *B*) Phagosomal cathepsin D/E (aspartic cathepsins) activities in resting BMMØs. (*C*–*F*) Phagosomal cathepsin B/L (cysteine cathepsins) activities in resting (*C* and *D*) and IFNγ-activated (*E* and *F*) BMMØs. (*A*, *C*, and *E*) Real-time representative traces. (*B*, *D*, and *F*) Averaged rates between 15 and 40 min postinternalization, relative to DMSO-treated WT samples, from three independent experiments. Error bars represent SEM. *P* values were determined by ANOVA. In contrast to increasing rates of cysteine cathepsin activity in the presence of an oxidative burst, quercetin and THF treatment delay onset and reduce initial rates of cysteine cathepsin activity in an "off-target" NOX2-independent fashion.

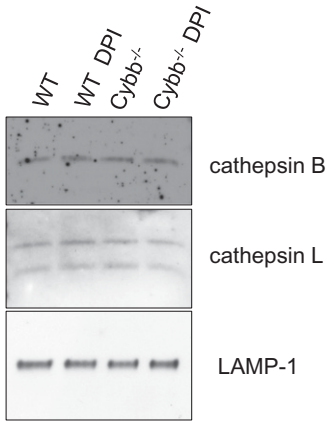

Fig. S6. Phagosomal delivery of cathepsins B and L is not affected by NOX2 activity. Images of Western blot depicting mature forms of cathepsin B and L and LAMP-1 in 30-min phagosomes magnetically isolated from WT and Cybb$^{-/-}$ BMMØs ± DPI (0.5 μM) treatment. Isolated phagosomes from each sample were standardized following enumeration with a hemocytometer. Western blotting was performed according to standard practices with chemiluminescent detection. Phagosomal preparations were evaluated for the enrichment of the lysosomal marker LAMP-1 and the absence of the endoplasmic reticulum marker protein disulfide isomerase.

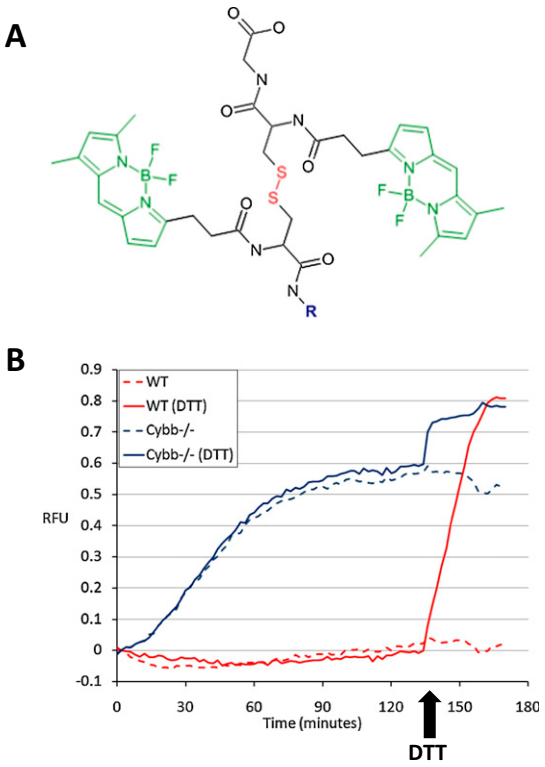

Fig. S7. Recording disulfide reduction in the phagosome using a particle-coupled cystine-based fluorometric substrate. The rates of phagosomal reduction of cystine (dimeric, oxidized form of two cysteine residues) were recorded by using a modified form of the self-quenched cystine-based fluorogenic substrate Bodipy FL L-cystine (Molecular Probes). (*A*) The final chemical structure of the cystine-based substrate. The Bodipy FL fluorophore groups are highlighted in green and the disulfide is in red. The R group represents an N-terminal or lysine side chain amino group of a protein covalently coupled to an experimental particle. Image was created using Symyx Draw 3.2 software. (*B*) The phagosomal reduction capacity assay showing substrate limitation approaching 2 h postinternalization in Cybb$^{-/-}$ BMMØs but no substrate limitation in WT macrophages. IFNγ-activated macrophages were given IgG-coupled experimental particles bearing the modified fluorogenic cystine-based reagent along with a calibration fluor (Alex Fluor 594 succinimidyl ester). At 125 min, cell-permeable disulfide-reducing agent dithiothreitol (DTT) (0.5 mM) was added to samples to fully reduce the fluorogenic substrate. RFU = SF_{RT}/CF_{RT} (where RFU = relative fluorescent units, SF_{RT} = substrate fluorescence in real time, and CF_{RT} = calibration fluorescence in real time).

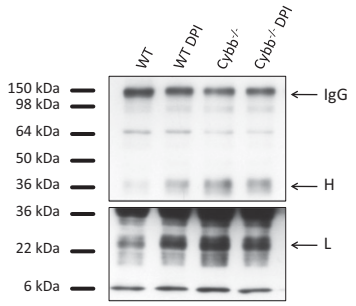

Fig. S8. NOX2 activity diminishes the capacity of the phagosome to reduce disulfide bonds between IgG subunits. Anti-BSA rat IgG was biotinylated with biotin succinimidyl ester, separated on a PD10 column (GE Healthcare), and used to opsonize 3-μm experimental particles covalently coated with BSA. Opsonized particles were washed and given to WT or Cybb$^{-/-}$ BMMØs with or without pretreatment with DPI (0.5 μM, 1 h), in the presence of 10 μg/mL leupeptin, 10 μM E64, 2 μg/mL pepstatin, and 10 μg/mL aprotinin to prevent IgG proteolysis. After 1 h at 37 °C, BMMØs were lysed in non-reducing sample buffer and separated by SDS/PAGE. Biotinylated holo-IgG (IgG), heavy (H) chain, and light (L) chain were identified by Western blot using streptavidin-horseradish peroxidase and standard chemiluminescent detection. The two panels are images of the same blot. A greater exposure was required to detect the band corresponding to the light chain (lower panel).

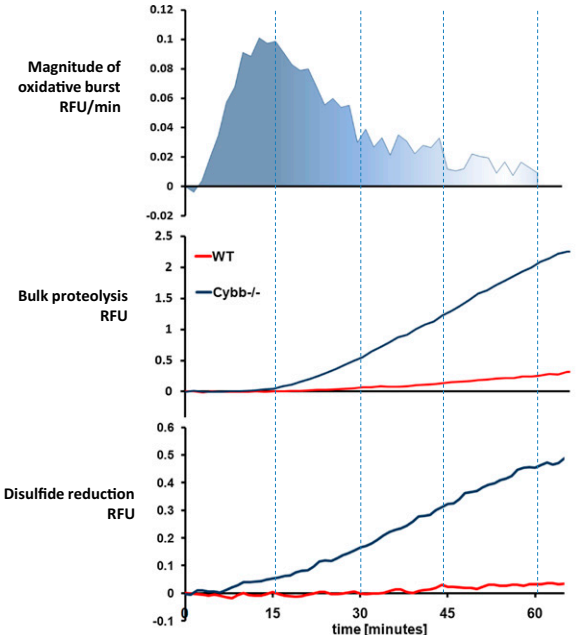

Fig. S9. NOX2- activity has a sustained effect on the reductive and proteolytic capacities of the phagosome. Representative traces of phagosomal bulk proteolysis and disulfide reduction in WT and Cybb$^{-/-}$ IFNγ-activated macrophages temporally aligned with the phagosomal oxidative burst. RFU = SF_{RT}/CF_{RT} (where RFU = relative fluorescent units, SF_{RT} = substrate fluorescence in real time, and CF_{RT} = calibration fluorescence in real time). The oxidative burst is expressed as RFU/min and thus correlates to the rate of H2HFF-OxyBURST substrate oxidation at a given point in time.